

Flatness-Based Motion Control of a UAV Slung Load System Using Quasi-Static Feedback Linearization

Zifei Jiang, Mohamed Al Lawati, Arash Mohammadhasani, and Alan F. Lynch

Abstract—This paper proposes an algorithm for deriving a quasi-static feedback for a general nonlinear differentially flat system. We apply this algorithm to design a quasi-static controller to track the payload position and yaw of a Unmanned Aerial Vehicle (UAV) multirotor Slung Load System (SLS). The design achieves full state feedback linearization of SLS with the important property that the control law is a static function of SLS state, i.e., no additional controller states are required as in full linearization achieved by the dynamic extension algorithm (DEA). The proposed controller ensures linear time-invariant exponentially stable error dynamics on a well-defined and practical region of state space. The design is validated in simulation.

I. INTRODUCTION

Load transport using Unmanned Aerial Vehicles (UAVs) has attracted interest in recent years. A survey of the results is in [1]. A Multirotor UAV Slung Load System (SLS) is one way of transporting payloads where a cable attached to the bottom of the UAV suspends the load. SLSs have a number of benefits including system maneuverability, keeping the payload at a safe distance from the vehicle, and providing a robust method of load transportation that can be generalized to multiple vehicles. Although SLSs are an attractive solution for load transport, developing a high performance and rigorous motion control is a challenge given the complex underactuated nonlinear dynamics involved. Developing a UAV SLS is part of a general recent trend that focuses on environment interaction, so-called Unmanned Aerial Manipulation [2, 3, 1].

The interest in UAV SLSs has led to a wealth of research on its motion control. Most of the work is based on a nonlinear UAV model coupled to a pendulum dynamics which describes the suspended load. In many cases controller design uses a multi-loop or inner-outer loop structure. Here, an outer loop controls the coupled translational UAV/pendulum dynamics. An inner loop controls the UAV's rotational degrees of freedoms (DoFs) using a reference from the outer loop. Examples of this approach include [4, 5, 6, 7]. Specifically, in [5, 6], a 3-loop control structure is proposed where the innermost loop tracks UAV attitude. The middle loop controls load attitude and UAV yaw. Finally, the outermost loop tracks load position. Exponential stability (ES) of the

nonlinear error dynamics is achieved on a local region which is difficult to describe and depends on controller gain.

Another nested control result is in [7]. Here, a partial feedback linearization is performed for the outer loop, while the inner-loop is fully feedback linearized. The method achieves exponential convergence of UAV position error and stabilization of the load angle. The design cannot be used for time-varying load position trajectory tracking and this limits the achievable motion.

Differential flatness is a property of nonlinear systems introduced in [8]. A survey of results is in [9]. A flat system possess so-called flat outputs which differentially parameterize the state and input. That is, we can express the state and input in terms of time derivatives of the flat output. This parameterization is often used for open-loop control design or motion planning. It is well-known that every flat system is linearizable by endogenous dynamic feedback [8]. An endogenous dynamic feedback is a particular kind of dynamic state feedback where controller state and auxiliary input can be expressed as a function of system state, system input and its time derivatives. The flatness property is preserved under this type of feedback [10]. In addition, every flat system can be linearized by quasi-static feedback [11]. Quasi-static feedback has the advantage of achieving linearization without augmenting the closed-loop dynamics with controller states as with dynamic state feedback [11].

Deriving complete necessary and sufficient conditions which can be used to construct a flat output remains an open problem. Only partial results are available and examples of recent work include [12] where the system dynamics is assumed to be a one-fold prolongation. Two-input systems and endogenous dynamic feedback are considered in [13]. Under typical modelling assumptions, the nonlinear SLS model has been shown to be flat in [6]. However, although that work used flatness for open-loop trajectory planning. There is no existing work on using flatness for *feedback* control of the SLS other than the companion paper [14] which applies the Dynamic Extension Algorithm (DEA) to derive a dynamic feedback linearization for output tracking. The benefit of using flatness for closed-loop control is that tracking error dynamics can be linearized and this simplifies the stability analysis. This should be compared to results in [6, 7] where stability analysis is complicated by the multi-loop controller structure.

The contribution of this paper is to describe a novel general algorithm, called the quasi-static feedback algorithm (QSFA), for computing a quasi-static state feedback. Such an algorithms does not appear in the literature to-date. As

Zifei Jiang, Mohamed Al Lawati, Arash Mohammadhasani, and Alan F. Lynch are with the Department of Electrical and Computer Engineering, University of Alberta, AB, T6G 2R3, CA. Email: {zifei.jiang, maallawa, Arash.Mhasani, alan.lynch}@ualberta.ca

Al Lawati is also with Dept. Mechanical & Industrial Engineering, Sultan Qaboos University, Muscat, Oman.

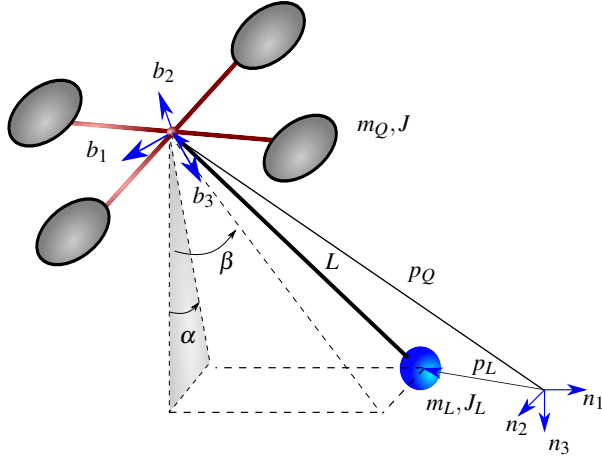


Fig. 1. The UAV with suspended load. The suspended load is modelled as a spherical pendulum attached to the UAV CoM.

well, our contribution is to apply the QSFA to the SLS. In a similar way to the DEA, the QSFA provides a straightforward procedure for testing whether a system is flat relative to a given output. This should be compared to the complicated conditions such as [12, 13] which apply to a restricted system class.

II. SLS MODELLING

This section presents the dynamic model for the SLS. The suspended load is modelled as a spherical pendulum attached to the UAV Centre of Mass (CoM). Table I and Fig. 1 gives some of the notation and variables used. Two references frames are used: a navigation frame \mathcal{N} and body frame \mathcal{B} . Frame \mathcal{N} is assumed inertial and has orthonormal basis vectors n_1, n_2, n_3 oriented north, east, and down, respectively. The origin of \mathcal{B} is the UAV's CoM and its basis vectors b_1, b_2, b_3 oriented (relative to the vehicle) forward, right, and down, respectively. The configuration space of the UAV SLS is $SE(3) \times \mathbb{S}^2$ which describes pendulum position p_L , UAV attitude R , and pendulum attitude q . The unit direction vector q of the load relative to \mathcal{N} is parameterized by two angles α and β . The angle of the pendulum about n_1 is α , and β is the angle about n_2 (see Fig. 1). We have

$$q = R_{n_1}(\alpha)R_{n_2}(\beta)n_3 = [s_\beta, -s_\alpha c_\beta, c_\alpha c_\beta]^T$$

where R_{n_1} and R_{n_2} are elementary rotation matrices about n_1 and n_2 axis, respectively.

The relation between load position p_L and quadrotor position p_Q is

$$p_L = p_Q + Lq = p_Q + L[s_\beta, -s_\alpha c_\beta, c_\alpha c_\beta]^T \quad (1)$$

where L is pendulum length. Differentiating (1), we obtain the velocity and acceleration relations

$$v_L = v_Q + L\dot{q} \quad (2)$$

$$\dot{v}_L = \dot{v}_Q + L\ddot{q} \quad (3)$$

TABLE I
SYMBOL SUMMARY

| Symbol | Description |
|---|---|
| $p_Q \in \mathbb{R}^3$ | position of UAV in \mathcal{N} |
| $p_L \in \mathbb{R}^3$ | position of load in \mathcal{N} |
| $v_Q = \dot{p}_Q \in \mathbb{R}^3$ | linear velocity of UAV in \mathcal{N} |
| $v_L = \dot{p}_L \in \mathbb{R}^3$ | linear velocity of load in \mathcal{N} |
| $R \in SO(3)$ | rotation matrix from \mathcal{N} to \mathcal{B} |
| $\eta = [\phi, \theta, \psi]^T \in \mathbb{R}^3$ | Euler angles parameterizing R |
| $q \in \mathbb{S}^2$ | orientation of the load |
| $[\alpha, \beta] \in \mathbb{R}^2$ | Euler angles parameterizing q |
| $[\gamma_\alpha = \dot{\alpha}, \gamma_\beta = \dot{\beta}] \in \mathbb{R}^2$ | time derivative of $[\alpha, \beta]$ |
| $\omega \in \mathbb{R}^3$ | angular velocity of UAV in \mathcal{B} |
| $\omega_L \in \mathbb{R}^3$ | angular velocity of load in \mathcal{N} |
| $\bar{u} \in \mathbb{R}_{\geq 0}$ | total thrust generated by the actuators |
| $\tau \in \mathbb{R}^3$ | propeller torque in \mathcal{B} |
| $T \in \mathbb{R}_{\geq 0}$ | tension in pendulum rod |
| $J, J_L \in \mathbb{R}^{3 \times 3}$ | inertia of UAV and load |
| L | length of the pendulum |
| m_Q, m_L | mass of UAV and load |
| g | gravitational acceleration |

The UAV dynamics is

$$\dot{p}_Q = v_Q \quad (4a)$$

$$m_Q \dot{v}_Q = m_Q g n_3 - R \bar{u} n_3 + T q \quad (4b)$$

$$\dot{R} = RS(\omega) \quad (4c)$$

$$J \dot{\omega} = -\omega \times J \omega + \tau \quad (4d)$$

where $J = \text{diag}(J_1, J_2, J_3) \in \mathbb{R}^{3 \times 3}$ is the inertia matrix of the UAV, $T \in \mathbb{R}_{\geq 0}$ denotes tension in the pendulum, $\bar{u} \in \mathbb{R}_{\geq 0}$ is the total propeller thrust, $\tau \in \mathbb{R}^3$ is propeller torque expressed in \mathcal{B} , g is acceleration due to gravity, and m_Q is UAV mass. The skew operator $S(\cdot) : \mathbb{R}^3 \rightarrow so(3)$ in (4c) is given by

$$S(x) = \begin{bmatrix} 0 & -x_3 & x_2 \\ x_3 & 0 & -x_1 \\ -x_2 & x_1 & 0 \end{bmatrix}, \quad \text{where } x = \begin{bmatrix} x_1 \\ x_2 \\ x_3 \end{bmatrix}.$$

The rotational kinematics in (4c) can be parameterized using the Euler angles $\eta = [\phi, \theta, \psi]^T \in \mathbb{R}^3$:

$$\dot{\eta} = W(\eta)\omega \quad (5)$$

with

$$W(\eta) = \begin{bmatrix} 1 & s_\phi t_\theta & c_\phi t_\theta \\ 0 & c_\phi & -s_\phi \\ 0 & s_\phi / c_\theta & c_\phi / c_\theta \end{bmatrix}$$

where $t_\theta = \tan \theta, s_\theta = \sin \theta, c_\theta = \cos \theta$.

For the pendulum translational dynamics we have

$$\dot{p}_L = v_L \quad (6)$$

$$m_L \dot{v}_L = -T q + m_L g n_3 \quad (7)$$

The rotational dynamics of the pendulum is

$$\dot{q} = \omega_L \times q \quad (8)$$

$$J_L \dot{\omega}_L = -\omega_L \times J_L \omega_L + L q \times (m_L g n_3 - m_L \dot{v}_Q) \quad (9)$$

where J_L is the load inertia matrix about the UAV CoM. Using Steiner's Theorem [15], we can express J_L as a function of relative position between the load and UAV:

$$J_L = m_L L^2 (I - q q^T) \quad (10)$$

Eliminating the internal force term T in (7) and (4b) we have

$$m_Q \dot{v}_Q + m_L \dot{v}_L = (m_Q + m_L)gn_3 - R\bar{u}n_3 \quad (11)$$

Substituting for \dot{v}_Q in (11) using (3), we have the translational dynamics for load position

$$\begin{aligned} (m_L + m_Q)\dot{v}_L &= (m_L + m_Q)gn_3 - R\bar{u}n_3 + m_Q L\ddot{q} \\ &= (m_L + m_Q)gn_3 - R\bar{u}n_3 \\ &\quad + m_Q L(\dot{\omega}_L \times q + \omega_L \times \dot{q}) \end{aligned} \quad (12)$$

where we have substituted $\ddot{q} = \dot{\omega}_L \times q + \omega_L \times \dot{q}$ from (8). Combining (12) and (3), we get the expression for \dot{v}_Q as:

$$\dot{v}_Q = -\frac{m_L}{m_Q + m_L}L\ddot{q} + gn_3 - \frac{R\bar{u}n_3}{m_Q + m_L} \quad (13)$$

Substituting (10), and (13) into (9), we obtain the rotational dynamics of the load expressed in \mathcal{N} :

$$\begin{aligned} m_Q L(I - qq^T)\dot{\omega}_L &= q \times R\bar{u}n_3 - m_L L(q^T \omega_L)\dot{q} \\ &\quad + (m_Q + m_L)L(q^T \omega_L)\omega_L \times q \end{aligned} \quad (14)$$

In addition, we have the relation between ω_L and $\gamma_\alpha, \gamma_\beta$

$$\omega_L = \begin{bmatrix} 1 \\ 0 \\ 0 \end{bmatrix} \gamma_\alpha + \begin{bmatrix} 0 \\ c_\alpha \\ s_\alpha \end{bmatrix} \gamma_\beta \quad (15)$$

and

$$\begin{aligned} \dot{\omega}_L &= \begin{bmatrix} 1 \\ 0 \\ 0 \end{bmatrix} \dot{\gamma}_\alpha + \begin{bmatrix} 0 \\ c_\alpha \\ s_\alpha \end{bmatrix} \dot{\gamma}_\beta + \begin{bmatrix} 0 \\ -s_\alpha \\ c_\alpha \end{bmatrix} \gamma_\alpha \gamma_\beta \\ &= R_{n_1}(\alpha) \begin{bmatrix} \dot{\gamma}_\alpha \\ \dot{\gamma}_\beta \\ \gamma_\alpha \gamma_\beta \end{bmatrix} \end{aligned} \quad (16)$$

Substituting (15) and (16) into (12) and (14), and solving for $\dot{v}_L, \dot{\gamma}_\alpha, \dot{\gamma}_\beta$, we obtain a state space form for the SLS dynamics

$$\dot{x} = \begin{bmatrix} v \\ \gamma_\alpha \\ \gamma_\beta \\ W(\eta)\omega \\ -\frac{s_\beta(\gamma_\alpha^2 c_\beta^2 + \gamma_\beta^2)Lm_Q}{m_Q + m_L} \\ \frac{s_\alpha c_\beta(\gamma_\alpha^2 c_\beta^2 + \gamma_\beta^2)Lm_Q}{m_Q + m_L} \\ g - \frac{c_\alpha c_\beta(\gamma_\alpha^2 c_\beta^2 + \gamma_\beta^2)Lm_Q}{m_Q + m_L} \\ 2\gamma_\alpha \gamma_\beta \mathfrak{t}_\beta \\ -\gamma_\alpha^2 c_\beta s_\beta \\ -J^{-1}S(\omega)J\omega \end{bmatrix} + \begin{bmatrix} 0_{8 \times 1} & 0_{8 \times 3} \\ \bar{g}(x) & 0_{5 \times 3} \\ 0_{3 \times 1} & J^{-1} \end{bmatrix} u \quad (17)$$

where

$$\begin{aligned} x &= [p_L^T, \alpha, \beta, \eta^T, v_L^T, \gamma_\alpha, \gamma_\beta, \omega^T]^T \in \mathbb{R}^{16} \\ u &= [\bar{u}, \tau^T]^T \in \mathbb{R}^4 \end{aligned}$$

and the expression for \bar{g} is given in the Appendix. We note that (17) has singularities at $c_\beta = c_\theta = 0$ due to

parametrization of the orientation of the UAV and pendulum. As a result, the domain \mathcal{M} of x is defined as a subset of \mathbb{R}^{16} that contains 0 but excludes these points. Practically, these singularities are unlikely to be of concern because they involve dangerous SLS motion. Furthermore, $c_\beta = 0$ would require the pendulum to collide with the UAV frame.

III. QUASI-STATIC FEEDBACK LINEARIZATION

We define the general system

$$\dot{x} = f(x) + \sum_{i=1}^m g_i(x)u_i \quad (18a)$$

$$y_i = h_i(x), \quad 1 \leq i \leq m \quad (18b)$$

with vector fields $f, g_i : \mathcal{M} \rightarrow \mathbb{R}^n$ and output functions $h_i : \mathcal{M} \rightarrow \mathbb{R}$ defined on an open subset $\mathcal{M} \subset \mathbb{R}^n$. The quasi-static feedback is taken as $u = u(x, v, \dot{v}, \ddot{v}, \dots, v^{(\rho)})$, where v is an auxiliary input which is eventually assigned to a linear function of the output tracking error and its time derivative. Compared with dynamic state feedback, quasi-static feedback is a static function of state, i.e., it requires no state augmentation. This leads to a simpler control design which is important for onboard implementation. In Section III-A we present the Quasi-Static Feedback Algorithm (QSFA) which produces a quasi-static feedback linearizing controller for a flat system of the form (18). The QSFA is then applied to the SLS in Section III-B.

A. Quasi-Static Feedback Algorithm (QSFA)

The Lie derivative of a function $\lambda : \mathcal{M} \rightarrow \mathbb{R}$ along the vector field f is defined by $L_f \lambda(x) = \frac{\partial \lambda}{\partial x} f(x)$. When performing QSFA, we make use of a vector of indices $r = [r_1, \dots, r_m]$ such that r_i is the largest integer satisfying $L_{g_j} L_f^{r_i} h_i(x) = 0, 1 \leq j \leq m, r_i < r_i - 1$, about some $x_0 \in \mathcal{M}$. The existence of these indices does not imply the system has a well-defined relative degree about x_0 as this requires the decoupling matrix

$$D(x) = \begin{bmatrix} L_{g_1} L_f^{r_1-1} h_1(x) & \dots & L_{g_m} L_f^{r_1-1} h_1(x) \\ \vdots & \dots & \vdots \\ L_{g_1} L_f^{r_m-1} h_m(x) & \dots & L_{g_m} L_f^{r_m-1} h_m(x) \end{bmatrix} \quad (19)$$

is nonsingular at x_0 .

Variables have superscript (i) to keep track of the algorithm iteration. Superscript (k) denotes the k th order time derivative. We begin with Step 0 and assume the decoupling matrix $D^{(0)} = D$ given by (19) has constant rank less than m about $x_0 \in \mathcal{M}$ where $r^{(0)} = [r_1^{(0)}, \dots, r_m^{(0)}]$. Define $s^{(i)} = \text{rank}(D^{(i)}(x_0))$, and $y^{(0)} = y^{(r^{(0)})} = [y_1^{(r_1^{(0)})}, \dots, y_m^{(r_m^{(0)})}]^T$.

Step 0: According to the definition of $r^{(0)}$ we can write $y^{(r^{(0)})}$ as

$$y^{(0)} = y^{(r^{(0)})} = a_0(x) + D^{(0)}u \quad (20)$$

We reorder and decompose $y^{(0)}$ as

$$y^{(0)} = \begin{bmatrix} \tilde{y}^{(0)} \\ \hat{y}^{(0)} \end{bmatrix} \quad (21)$$

where $\hat{y}^{(0)}$ corresponds to the first $s^{(0)}$ independent rows of $D^{(0)}$. Introducing auxiliary inputs $v_1 = \hat{y}^{(0)}$ and since the last rows of $D^{(0)}$ are linearly dependent on the first $s^{(0)}$ rows, we can write

$$\hat{y}^{(0)} = \tilde{a}_0(x) + \tilde{b}_0(x)u = v_1 \quad (22)$$

$$\hat{y}^{(0)} = \hat{y}^{(0)}(x, v_1) \quad (23)$$

where $\hat{y}^{(0)}$ is affine in v_1 and $\tilde{b}_0(x)$ are the first $s^{(0)}$ independent rows of $D^{(0)}$. Similarly, the index $r^{(1)}$ is calculated by taking the time derivative of $\hat{y}^{(0)}$. We obtain

$$\dot{\hat{y}}^{(0)} = \hat{y}^{(r^{(0)}+1)} = \frac{\partial \hat{y}^{(0)}}{\partial x} [f(x) + \sum_{i=1}^m g_i(x)u_i] + \frac{\partial \hat{y}^{(0)}}{\partial v_1} \dot{v}_1 \quad (24)$$

$$\begin{aligned} &= L_f \hat{y}^{(0)} + \frac{\partial \hat{y}^{(0)}}{\partial v_1} \dot{v}_1 + \sum_{i=1}^m L_{g_i} \hat{y}^{(0)} u_i \\ &= a_1(x, v_1) + b_1(x)u \end{aligned} \quad (25)$$

where $b_1(x) \in \mathbb{R}^{(m-s^{(0)}) \times m}$ is given by

$$b_1(x) = \begin{bmatrix} L_{g_1} \hat{y}_1^{(0)}(x) & \dots & L_{g_m} \hat{y}_1^{(0)}(x) \\ \vdots & \dots & \vdots \\ L_{g_1} \hat{y}_{m-s^{(0)}}^{(0)}(x) & \dots & L_{g_m} \hat{y}_{m-s^{(0)}}^{(0)}(x) \end{bmatrix} \quad (26)$$

Three different cases may appear. If $b_1(x)$ is identically zero, we should continue to take the time derivative of $\hat{y}^{(0)}$. If any row of $b_1(x)$ is linearly dependent on $\tilde{b}_0(x)$ in (22), it should be expressed by (x, v_1) similar to (23), and then time derivatives of these rows should be taken. If all rows of $b_1(x)$ are linearly independent of $\tilde{b}_0(x)$ in (22). Define $r^{(1)} = [r_1^{(1)}, \dots, r_{m-s^{(0)}}^{(1)}]$ so that we have $y^{(1)} = (\hat{y}^{(0)})^{(r^{(1)})}$. Every row of the corresponding decoupling matrix $D^{(1)}$ is linearly independent of every row of $\tilde{b}_0(x)$. Decompose $y^{(1)}$ as

$$y^{(1)} = \begin{bmatrix} \tilde{y}^{(1)} \\ \hat{y}^{(1)} \end{bmatrix} \quad (27)$$

where $\tilde{y}^{(1)}$ corresponds to the first $s^{(1)}$ independent rows of $D^{(1)}$. Introducing auxiliary inputs $v_2 = \tilde{y}^{(1)}$. Similar to (22) and (23), $y^{(1)}$ can be written as

$$\tilde{y}^{(1)} = \tilde{a}_1(x, v_1, \dots, v_1^{(r^{(1)})}) + \tilde{b}_1(x, v_1, \dots, v_1^{(r^{(1)}-1)})u = v_2 \quad (28)$$

$$\hat{y}^{(1)} = \hat{y}^{(1)}(x, v_1, \dots, v_1^{(r^{(1)})}, v_2) \quad (29)$$

Step $k+1$. Suppose that in Steps 0 through k , $y^{(0)}, \dots, y^{(k)}$ have been defined so that

$$\hat{y}^{(0)} = \tilde{a}_0(x) + \tilde{b}_0(x)u$$

\vdots

$$\hat{y}^{(k)} = \tilde{a}_k(x, \{v_i^{(j)} | 1 \leq i \leq k, 1 \leq j \leq \sum_{l=1}^k r^{(l)}\})$$

$$+ \tilde{b}_k(x, \{v_i^{(j)} | 1 \leq i \leq k, 1 \leq j \leq \sum_{l=1}^k r^{(l)} - 1\})u$$

$$\hat{y}^{(k)} = \hat{y}_k^{(k)}(x, \{v_i^{(j)} | 1 \leq i \leq k, 1 \leq j \leq \sum_{l=1}^k r^{(l)}\}, v_{k+1})$$

and so that they are rational functions of $v_i^{(j)}$. Define $y^{(k+1)} = (\hat{y}^{(r^{(k)})})^{(r^{(k+1)})}$ which can be decomposed as before:

$$y^{(k+1)} = \begin{bmatrix} \tilde{y}^{(k+1)} \\ \hat{y}^{(k+1)} \end{bmatrix} \quad (30)$$

where $\tilde{y}^{(k+1)}$ consist of the first $s^{(k+1)}$ independent rows of $D^{(k+1)}$. Introducing auxiliary inputs $v_{k+2} = \tilde{y}^{(k+1)}$, (30) can be written as

$$\tilde{y}^{(k+1)} = \tilde{a}_{k+1}(x, \{v_i^{(j)} | 1 \leq i \leq k+1, 1 \leq j \leq \sum_{l=1}^{k+1} r^{(l)}\})$$

$$+ \tilde{b}_k(x, \{v_i^{(j)} | 1 \leq i \leq k+1, 1 \leq j \leq \sum_{l=1}^{k+1} r^{(l)} - 1\})u$$

$$\hat{y}^{(k+1)} = \hat{y}_{k+1}^{(k)}(x, \{v_i^{(j)} | 1 \leq i \leq k+1, 1 \leq j \leq \sum_{l=1}^{k+1} r^{(l)}\}, v_{k+2})$$

If $s^{(0)} + s^{(1)} + \dots + s^{(k+1)} = m$, the algorithm terminates. Otherwise, we take the time derivative of $\hat{y}^{(k+1)}$ and perform the next iteration.

Defining $[\tilde{y}^{(0)}, \dots, \tilde{y}^{(k+1)}]^T = [v_1, \dots, v_{k+2}]^T = v \in \mathbb{R}^m$, and when the algorithm terminates, we have an invertible relation between the original input u and auxiliary input v :

$$v = \begin{bmatrix} \tilde{a}_0(x) \\ \vdots \\ \tilde{a}_{k+1}(x, \{v_i^{(j)} | 1 \leq i \leq k+1, 1 \leq j \leq \sum_{l=1}^{k+1} r^{(l)}\}) \end{bmatrix} + D^o u$$

where D^o is the final decoupling matrix with $\text{rank}(D^o) = m$.

B. SLS Controller Design Using QSFA

In this section, the QSFA is applied to the 16-dimensional SLS model (17). It is shown that the SLS can be quasi-static state feedback linearized using QSFA and the pendulum position and yaw as outputs y ,

$$y = [p_L^T, \psi]^T \quad (31)$$

Step 0. According to (19), we have

$$D^{(0)} = \begin{bmatrix} d_{11}^{(0)} & 0 & 0 & 0 \\ d_{21}^{(0)} & 0 & 0 & 0 \\ d_{31}^{(0)} & 0 & 0 & 0 \\ 0 & 0 & \frac{s_\phi}{J_2 c_\theta} & \frac{c_\phi}{J_3 c_\theta} \end{bmatrix} \quad (32)$$

where d_{11}, d_{21}, d_{31} are functions of state and the index $r^{(0)} = [2, 2, 2, 2]^T$ and $\text{rank}(D^{(0)}) = 2$ on a subset of \mathcal{M} where

$$d_{31}^{(0)}(x) = -\frac{[s_\beta, -s_\alpha c_\beta, c_\alpha c_\beta] \cdot Rn_3}{m_Q + m_L} \neq 0 \quad (33)$$

Referring to (20), we have

$$y^{(0)} = a_0(x) + D^{(0)}u \quad (34)$$

Thus $y^{(0)}$ is decoupled as $\tilde{y}^{(0)} = [\ddot{y}_3, \ddot{y}_4]^T$, and $\hat{y}^{(0)} = [\ddot{y}_1, \ddot{y}_2]^T$. Here, we introduce auxiliary input $v_1 = [\ddot{y}_3, \ddot{y}_4]^T$, we have

$$v_1 = \tilde{y}^{(0)} = \tilde{a}_0(x) + \tilde{b}_0(x)u \quad (35)$$

Then, $\hat{y}^{(0)}$ in (23) can be written as

$$\hat{y}^{(0)} = \begin{bmatrix} -(g - [1, 0]^T v_1) t_\beta / c_\alpha \\ (g - [1, 0]^T v_1) t_\alpha \end{bmatrix} \quad (36)$$

Step 1. Taking a time derivative of $\hat{y}^{(0)}$ we obtain

$$\dot{\hat{y}}^{(0)} = \begin{bmatrix} \frac{\dot{v}_1 s_\beta}{c_\beta c_\alpha^2} - \frac{\gamma_\beta (g - v_1)}{c_\beta^2 c_\alpha} - \frac{\gamma_\alpha s_\alpha s_\beta (g - v_1)}{c_\beta c_\alpha} \\ -\dot{v}_1 t_\alpha + \frac{\gamma_\alpha (g - v_1)}{c_\alpha^2} \end{bmatrix} \quad (37)$$

Taking the second time derivative of $\hat{y}^{(0)}$ gives

$$\ddot{\hat{y}}^{(0)} = a_1(x, v_1, \dot{v}_1, \ddot{v}_1) + b_1(x, v_1, \dot{v}_1)u \quad (38)$$

where $a_1(x, v_1, \dot{v}_1, \ddot{v}_1) \in \mathbb{R}^{2 \times 1}$, $b_1(x, v_1, \dot{v}_1) \in \mathbb{R}^{2 \times 4}$ are functions of x , auxiliary input v , and its time derivative. The matrix b_1 has the structure

$$b_1(x, v_1, \dot{v}_1) = \begin{bmatrix} b_{11} & 0 & 0 & 0 \\ b_{21} & 0 & 0 & 0 \end{bmatrix} \quad (39)$$

We observe that both rows of (39) are linearly dependent on the third row of $D^{(0)}$, thus $\ddot{\hat{y}}^{(0)}$ can be expressed using v_1 . As a result, (38) can be written as $\ddot{\hat{y}}^{(0)} = \ddot{\hat{y}}^{(0)}(x, v_1, \dot{v}_1, \ddot{v}_1)$ with input u eliminated. The same procedure is applied for $(\hat{y}^{(0)})^{(3)}$. When we calculate $(\hat{y}^{(0)})^{(4)}$, the corresponding decoupling matrix $D^{(1)}$ is

$$D^{(1)} = \begin{bmatrix} d_{11}^{(1)} & d_{12}^{(1)} & d_{13}^{(1)} & 0 \\ d_{21}^{(1)} & d_{22}^{(1)} & d_{23}^{(1)} & 0 \end{bmatrix} \quad (40)$$

where $d_{ij}^{(1)}$ are functions of $(x, v_1, \dots, v_1^{(3)})$ with $\text{rank}(D^{(1)}) = 2$ and its rows are linear independent of any row in $D^{(0)}$. Thus, we get $r^{(1)} = [4, 4]$. Introducing the auxiliary input $v_2 = (\hat{y}^{(0)})^{(r^{(1)})} = y^{(1)}$, we have

$$v_2 = y^{(1)} = \tilde{a}_1(x, v_1, \dots, v^{(4)}) + D^{(1)}u \quad (41)$$

Combining v_1 and v_2 , we have an invertible relation between the original input u and auxiliary inputs v_1 and v_2 .

$$\begin{bmatrix} v_1 \\ v_2 \end{bmatrix} = \begin{bmatrix} \tilde{a}_0(x) \\ \tilde{a}_1(x, v_1, \dots, v^{(4)}) \end{bmatrix} + D^o u \quad (42)$$

where D^o is the final decoupling matrix with $\text{rank}(D^o) = 4$ given below

$$D^o = \begin{bmatrix} d_{31}^{(0)} & 0 & 0 & 0 \\ 0 & 0 & \frac{s_\phi}{J_2 c_\theta} & \frac{c_\phi}{J_3 c_\theta} \\ d_{11}^{(1)} & d_{12}^{(1)} & d_{13}^{(1)} & 0 \\ d_{21}^{(1)} & d_{22}^{(1)} & d_{23}^{(1)} & 0 \end{bmatrix} \quad (43)$$

C. Output Tracking

By setting $[v_1, v_2]^T = [y_3^{(2)}, y_4^{(2)}, y_1^{(6)}, y_2^{(6)}]^T$ as in (42), a quasi-static feedback linearizing controller law is obtained. The tracking error is defined as

$$\begin{aligned} \tilde{z} = & [y_1 - y_{d1}, \dot{y}_1 - \dot{y}_{d1}, \dots, y_1^{(5)} - y_{d1}^{(5)}, \\ & y_2 - y_{d2}, \dot{y}_2 - \dot{y}_{d2}, \dots, y_2^{(5)} - y_{d2}^{(5)}, \\ & y_3 - y_{d3}, \dot{y}_3 - \dot{y}_{d3}, y_4 - y_{d4}, \dot{y}_4 - \dot{y}_{d4}]^T \end{aligned} \quad (44)$$

where $y_{di}, 1 \leq i \leq 4$ are desired outputs. The variables $y_1^{(3)}, \dots, y_1^{(5)}$, and $y_2^{(3)}, \dots, y_2^{(5)}$ are functions of $x, v_1, \dot{v}_1, \dots, v_1^{(4)}$, while the remaining outputs and their derivatives in (44) can be expressed as a function of x .

We can express the dynamics in the \tilde{z} -coordinates as

$$\dot{\tilde{z}} = A_c \tilde{z} + B_c (\tilde{a} + D^o u) \quad (45)$$

where

$$\begin{aligned} A_c &= \text{diag}(A_1, A_2, A_3, A_4) \\ B_c &= [e_6 \quad e_{12} \quad e_{14} \quad e_{16}] \\ \tilde{a} &= [\tilde{a}_0(x), \tilde{a}_1(x, v_1, \dots, v^{(4)})]^T \end{aligned}$$

$e_i \in \mathbb{R}^{16}$ denotes the unit vector in the i th direction, and

$$A_1 = A_2 = \begin{bmatrix} 0 & 1 \\ 0 & 0 \end{bmatrix}, \text{ and } A_j = \begin{bmatrix} 0_{5 \times 1} & I_5 \\ 0 & 0_{1 \times 5} \end{bmatrix} \in \mathbb{R}^{6 \times 6}$$

with $j = 3, 4$. Applying the linearizing control $u = D^{o-1}(K\tilde{z} - \tilde{a} + y_d^{(r)})$ with $y_d^{(r)} = [y_{d1}^{(6)}, y_{d2}^{(6)}, y_{d3}^{(2)}, y_{d4}^{(2)}]^T$ to (45) gives

$$\dot{\tilde{z}} = (A_c + B_c K) \tilde{z} \quad (46)$$

where $K \in \mathbb{R}^{4 \times 16}$ is the control gain chosen so that $A_c + B_c K$ is Hurwitz and the tracking error transient performance is satisfactory. Because $\dot{v}_1, \dots, v_1^{(4)}$ are calculated using $y_3 - y_{d3}, \dot{y}_3 - \dot{y}_{d3}, y_4 - y_{d4}, \dot{y}_4 - \dot{y}_{d4}$ and their time derivatives, the controller depends only on x and the reference trajectory. Hence, it is a static state feedback.

D. Domain of the Dynamic State Feedback Linearization

In this section, we determine the domain on which the quasi-static control law is well-defined. The control is singular at $\theta = \pm 90^\circ$ and $\beta = \pm 90^\circ$ as these are singularities occur in the SLS model due to Euler angles. At points where the Jacobian matrix of the \tilde{z} -coordinates is singular, the control is also singular. These are the same points as those where the distribution rank condition [16] does not hold. Alternatively, we can find these points from singularities in the decoupling matrix D^o in (43). We have,

$$\phi = \pm 90^\circ \quad (47a)$$

$$[s_\beta, -s_\alpha c_\beta, c_\alpha c_\beta] \cdot Rn_3 = 0 \quad (47b)$$

$$\ddot{p}_3 = g - \frac{c_\alpha c_\beta (\gamma_\alpha^2 c_\beta^2 + \gamma_\beta^2) Lm}{m_Q + m_L} \quad (47c)$$

$$\ddot{p}_3 = g \quad (47d)$$

We note that the geometric interpretation of the left-hand-side (LHS) of (47b) (which is a scaling of a_{31} from (33)) is the inner product of $q = [s_\beta, -s_\alpha c_\beta, c_\alpha c_\beta]$ and the direction of the thrust vector Rn_3 . Thus, when the direction of the pendulum is perpendicular to the thrust vector, a physical singularity occurs. The condition (47c) corresponds to $\ddot{u} = 0$. When the pendulum's downward linear acceleration $\ddot{p}_3 = g$, we obtain (47d). This is another physical singularity that often appears in a UAV motion control, e.g., [17]. Hence, we conclude that the controller's domain is a reasonable subset of \mathcal{M} that excludes the aforementioned points which are not typical of normal operation.

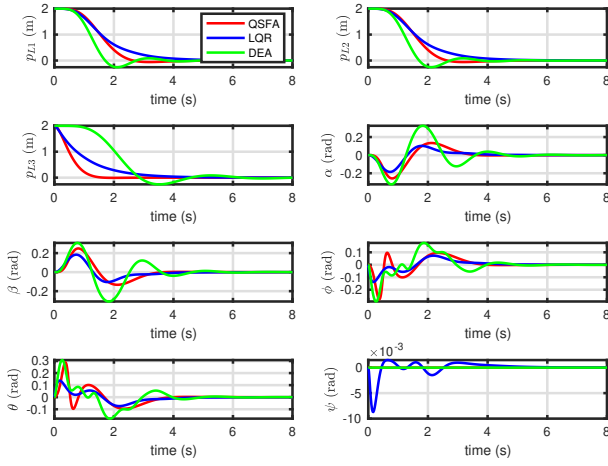


Fig. 2. System states p_L, α, β, η .

IV. SIMULATION

In this section, the quasi-static control law is validated using simulation. We consider simulations for output stabilization and tracking. Table II contains the system parameters used in the model and controller.

The quasi-static controller from the QSFA is compared with the dynamic state feedback linearizing controller obtained from the DEA [18, 14]. As well, we compare the design with a traditional linear LQR controller based on an approximate linearization at the origin. Both QSFA and DEA controllers have linear error dynamics. The advantage of quasi-static feedback is that it avoids dynamics in the controller. This makes quasi-static feedback easier implement as no discretization of dynamics is required.

TABLE II
SYSTEM PARAMETERS.

| | |
|-------|--------------------------|
| m | 1.6 kg |
| m_p | 0.16 kg |
| L | 1 m |
| J_1 | 0.03 kg · m ² |
| J_2 | 0.03 kg · m ² |
| J_3 | 0.03 kg · m ² |

Position Stabilization This section considers stabilization of the SLS at $x = 0$. The system is initialised with $p_L(0) = [2, 2, 2]^T$ m and the remaining states are set to zero (i.e., the SLS is at rest). The control gain for the LQR control is based on $Q = 100 \cdot I_{16}, R = 0.1 \cdot I_4$, where I_n is the $n \times n$ identity matrix. Given that the error dynamics (46) is linear time invariant (LTI), designing the transient performance for y is straightforward. Figs. 3, and 2 show the control input and configuration variables. The LQR controller exhibits similar transient error performance to the quasi-static control. However, LQR control results in large control input transients near $t = 0$. The dynamic state feedback linearization results in similar performance to the quasi-static control.

Trajectory Tracking: The proposed QSFA controller is capable of tracking complex reference trajectories. We consider

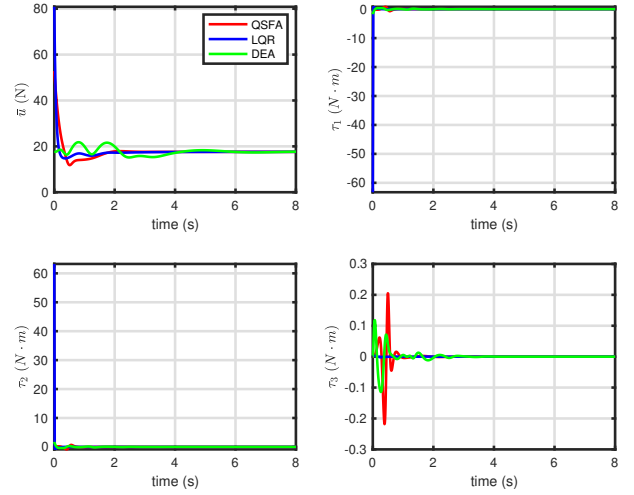


Fig. 3. Inputs \bar{u}, τ .

the “figure-8” reference

$$y_d(t) = \begin{bmatrix} 3 \sin(\pi t/4) + 1 \\ 1.5 \sin(\pi t/2) \\ 4 \sin(\pi t/4) - 4 \\ 0.02t \end{bmatrix} \quad (48)$$

The tracking error is shown in Fig. 4 and the configuration variables are shown in Fig. 5. The input trajectories are given in Fig. 6. We observe that tracking error converges to 0 with a fast transient and small overshoot. Input trajectories remain within a practical range. The gain for the QSFA and DEA controllers were obtained using LQR. The QSFA and DEA controls have similar performance. However, since the DEA controller is dynamic, it requires more computation.

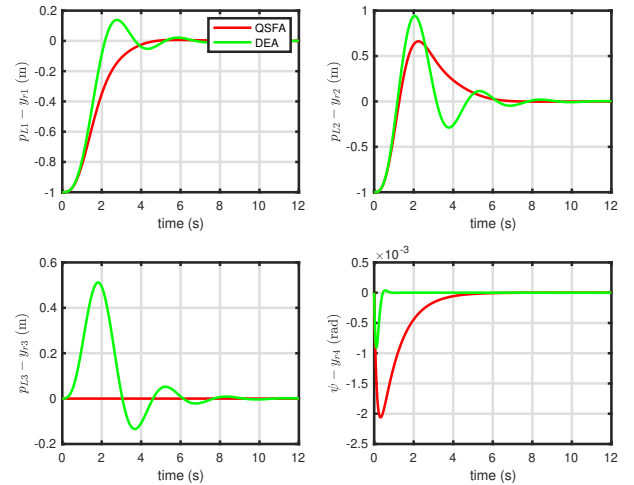


Fig. 4. Output tracking error $y - y_d$.

V. CONCLUSIONS

This paper presents a novel algorithm for deriving a quasi-static feedback controller for a general a flat system. The algorithm is applied to a SLS. The design leads to LTI

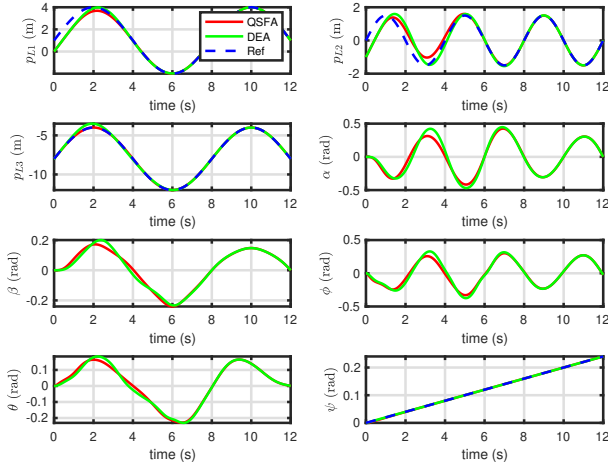


Fig. 5. System states p, α, β, η .

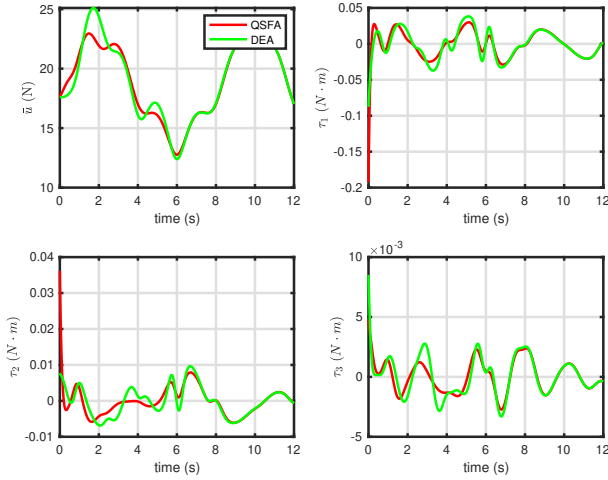


Fig. 6. Inputs \bar{u}, τ .

exponentially stable pendulum error dynamics on a well-defined and practical region of state space. Although the QSFA is investigated in [19, 20, 21], the design procedure is only demonstrated by example. This paper is the first to provide an algorithm for quasi-static control. The procedure for applying the QSFA is described in detail for the SLS. Simulations illustrate improved performance relative to a linear state feedback. Similar performance is obtained relative to a dynamic feedback linearization. However, the QSFA control requires less computation and no time-discretization, making it more suitable for on-board implementation.

APPENDIX

The expression for $\bar{g}(x)$ is

$$\bar{g}(x) = M^{-1}B = \begin{bmatrix} -\frac{\xi_1 + \xi_2 s_\beta^2}{m_Q + m_L} \\ \frac{(\xi_3 + \xi_4)c_\beta}{m_Q + m_L} \\ \frac{(\xi_5 - \xi_6)c_\alpha c_\beta}{m_Q + m_L} \\ \frac{\xi_7}{Lm_Q c_\beta} \\ \frac{\xi_8 + \xi_9}{Lm_Q} \end{bmatrix}$$

where

$$\begin{aligned} \xi_1 &= c_\beta s_\beta ((c_\alpha c_\theta - s_\alpha s_\theta s_\psi) c_\phi + c_\psi s_\alpha s_\phi) \\ \xi_2 &= c_\phi s_\theta c_\psi + s_\phi s_\psi \\ \xi_3 &= c_\beta ((c_\alpha^2 s_\theta s_\psi + c_\alpha c_\theta s_\alpha - s_\psi s_\theta) c_\phi + c_\psi s_\phi s_\alpha^2) \\ \xi_4 &= s_\beta s_\alpha (c_\phi s_\theta c_\psi + s_\phi s_\psi) \\ \xi_5 &= c_\beta ((s_\alpha s_\theta s_\psi - c_\alpha c_\theta) c_\phi - c_\psi s_\alpha s_\phi) \\ \xi_6 &= s_\beta (c_\phi s_\theta c_\psi + s_\phi s_\psi) \\ \xi_7 &= c_\psi c_\alpha s_\phi - c_\phi (s_\theta c_\alpha s_\psi + s_\alpha c_\theta) \\ \xi_8 &= c_\phi (s_\beta (s_\alpha s_\theta s_\psi - c_\alpha c_\theta) + c_\beta c_\psi s_\theta) \\ \xi_9 &= s_\phi (c_\beta s_\psi - c_\psi s_\alpha s_\beta) \end{aligned}$$

REFERENCES

- [1] D. K. D. Villa, A. S. Brandão, and M. Sarcinelli-Filho, "A survey on load transportation using multi-rotor UAVs," *Journal of Intelligent & Robotic Systems*, vol. 98, no. 2, pp. 267–296, 2020.
- [2] H. B. Khamseh, F. Janabi-Sharifi, and A. Abdessameud, "Aerial manipulation—a literature survey," *Robotics and Autonomous Systems*, vol. 107, pp. 221–235, 2018.
- [3] F. Ruggiero, V. Lippiello, and A. Ollero, "Aerial manipulation: A literature review," *IEEE Robotics and Automation Letters*, vol. 3, no. 3, pp. 1957–1964, 2018.
- [4] K. Klausen, T. I. Fossen, and T. A. Johansen, "Nonlinear control with swing damping of a multirotor UAV with suspended load," *Journal of Intelligent & Robotic Systems*, vol. 88, no. 2-4, pp. 379–394, 2017.
- [5] K. Sreenath, N. Michael, and V. Kumar, "Trajectory generation and control of a quadrotor with a cable-suspended load - a differentially-flat hybrid system," in *Proceedings of the IEEE International Conference on Robotics and Automation*, Karlsruhe, Germany, May 2013.
- [6] K. Sreenath, T. Lee, and V. Kumar, "Geometric control and differential flatness of a quadrotor UAV with a cable-suspended load," in *Proceedings of the 52nd IEEE Conference on Decision and Control*, Firenze, Italy, Dec. 2013.
- [7] S. Yang and B. Xian, "Exponential regulation control of a quadrotor unmanned aerial vehicle with a suspended payload," *IEEE Transactions on Control System Technology*, vol. 28, no. 6, pp. 2762–2769, 2020.
- [8] M. Fliess, J. Lévine, P. Martin, and P. Rouchon, "Flatness and defect of non-linear systems: introductory theory and examples," *International Journal of Control*, vol. 61, no. 6, pp. 1327–1361, 1995.
- [9] P. Martin, R. Murray, and P. Rouchon, "Flat systems," *Plenary Lectures and Mini-Courses 4th European Control Conference*, pp. 1–55, 1997.
- [10] J. Rudolph, *Flatness-based control: an introduction*. Shaker Verlag, 2021.
- [11] E. Delaleau and J. Rudolph, "Control of flat systems by quasi-static feedback of generalized states," *International Journal of Control*, vol. 71, no. 5, pp. 745–765, 1998.

- [12] F. Nicolau and W. Respondek, "Flatness of multi-input control-affine systems linearizable via one-fold prolongation," *SIAM Journal on Control and Optimization*, vol. 55, no. 5, pp. 3171–3203, 2017.
- [13] C. Gstöttner, B. Kolar, and M. Schöberl, "Necessary and sufficient conditions for the linearisability of two-input systems by a two-dimensional endogenous dynamic feedback," *International Journal of Control*, pp. 1–22, 2021, online access.
- [14] A. Mohammadhasani, M. Al Lawati, Z. Jiang, and A. F. Lynch, "Dynamic feedback linearization of a uav suspended load system," in *Proceedings of the International Conference on Unmanned Aircraft Systems*, Dubrovnik, Croatia, Jun. 2022.
- [15] K. M. Lynch and F. C. Park, *Modern robotics*. Cambridge University Press, 2017.
- [16] H. Nijmeijer and J. Schumacher, "The regular local noninteracting control problem for nonlinear control systems," *SIAM Journal on Control and Optimization*, vol. 24, no. 6, pp. 1232–1245, 1986.
- [17] A. Moeini, A. F. Lynch, and Q. Zhao, "A backstepping disturbance observer control for multirotor uavs: theory and experiment," *International Journal of Control*, pp. 1–15, 2021, online access.
- [18] H. Nijmeijer and W. Respondek, "Dynamic input-output decoupling of nonlinear control systems," *IEEE Transactions on Automatic Control*, vol. 33, no. 11, pp. 1065–1070, 1988.
- [19] J. Rudolph and E. Delaleau, "Some remarks on quasi-static feedback of generalized states," in *New Trends in Design of Control Systems*. Elsevier, 1994, no. 11, pp. 51–56.
- [20] E. Delaleau and J. Rudolph, "Some examples and remarks on quasi-static feedback of generalized states," *Automatica*, vol. 34, no. 8, pp. 993–999, 1998.
- [21] O. Fritsch, P. D. Monte, M. Buhl, and B. Lohmann, "Quasi-static feedback linearization for the translational dynamics of a quadrotor helicopter," in *Proceedings of the American Control Conference*, Montreal, QC, Canada, Jun. 2012.